Journal of Sailing Technology 2025, volume 10, issue 1, pp. 429 – 461.
The Society of Naval Architects and Marine Engineers.

The Intact Stability of Wind-Assisted Merchant Vessels

Pablo Albers
Fraunhofer WG Sustainable Maritime Mobility, Emden/Leer University of Applied Sciences, Germany, pablo.albers@hs-emden-leer.de.

Michael Vahs
Fraunhofer WG Sustainable Maritime Mobility, Emden/Leer University of Applied Sciences, Germany.

Manuscript received October 5, 2025; revision received December 3, 2025; accepted December 15, 2025.

Abstract. Wind-Assisted Propulsion Systems (WAPS) are increasingly being considered as a viable solution to reduce the fuel consumption and harmful emissions of merchant vessels, and both system size and the number of installations are steadily growing. A critical factor to safely exploit these systems is the vessel's stability, which classification societies ensure through the use of additional minimum stability criteria for WAPS-equipped vessels. In contrast to those for motor vessels, for which the International Maritime Organization specifies standardised minimum criteria, there is no harmonised approach. This paper presents the results from a master thesis study analysing the intact stability of WAPS-equipped vessels and these existing additional criteria. It encompassed four types of WAPS from two distinct categories, evaluating intact and dynamic stability criteria and underlying calculation methods and assumptions, in which notable gaps and inconsistencies were observed. The operational characteristics of WAPS were covered as well; it was observed that these can have a significant impact on the stability risk, an aspect not always adequately accounted for, and that the differences between mechanical and conventional WAPS are significant. The study has demonstrated that the various operational and physical characteristics of WAPS are not comprehensively addressed by current stability standards. To ensure suitability for their purpose the additional stability criteria for WAPS-equipped vessels require further development and refinement, keeping in mind both harmonisation and clarity. The adoption of system specific criteria should be explored. This will support the advancement of wind propulsion technology on merchant vessels by enabling a safe increase in system size and efficiency, while also facilitating regulatory compliance.

Keywords: Wind Assisted Propulsion Systems; Intact Stability; Dynamic Stability; Stability Criteria; WAPS Operational Risks; Sailing Cargo Vessels; WAPS Stability Standards.

NOMENCLATURE

A	WAPS wind area [m^2]
A_{a-b}	Area under the stability curve between $\theta = a$ and $\theta = b$ in meter radians [m rad]
A_R	Aspect Ratio [-]
C_D	Aerodynamic drag force coefficient acting parallel to the apparent wind direction [-]
C_H	Wind pressure height coefficient [-]
C_L	Aerodynamic lift force coefficient acting perpendicular to the apparent wind direction [-]
C_q	Suction coefficient [-]
C_Y	Side force coefficient acting laterally to the vessel in the Y-direction [-]
F_D	Aerodynamic drag force acting perpendicular to the apparent wind direction [t]
F_L	Aerodynamic lift force acting perpendicular to the apparent wind direction [t]
F_{water}	Hydrodynamic underwater force acting in the CLR opposite to F_Y [t]
F_Y	Side force acting laterally to the vessel in the Y-direction [t]
G_f	Gust factor [-]

$\overline{GM}_0$ Initial metacentric height [m]
$\overline{GZ}$ Righting lever [m]
$\overline{GZ}_{a^\circ}$ GZ at $\theta = a$ [m]
$\overline{GZ}_{\max}$ Maximum value of $\overline{GZ}$ [m]
H Heeling arm [m]
H_0 Vertical distance between the wind area centroid and a point at mid-draft [m]
l_{w1} Steady wind heeling lever [m]
l_{w2} Gust wind heeling lever [m]
M_H Wind heeling moment [t m]
M_R Righting moment [t m]
P Wind pressure [Pa]
Q Volumetric suction flow of suction sail [m^3 s^{-1}]
S_R Flettner rotor speed ratio describing the rotor's tangential velocity relative to V_A [-]
T Vessel draft [m]
V_A Apparent wind velocity [m s^{-1}]
V_{ref} Reference wind velocity [m s^{-1}]
V_S Vessel speed [m s^{-1}]
V_T True wind velocity [m s^{-1}]
V_z Actual wind velocity [m s^{1}]
z Height of V_z [m]
Z Upright heeling arm between the CE and the CLR [m]
Z_0 Vertical distance between the wind area centroid and a point at mid-draft in RINA criteria [m]
z_{ref} Height of V_{ref} [m]
Z_w Heeling arm in RINA's additional stability criteria for WAPS [m]

α Sail's angle of attack [deg]
β Apparent wind direction relative to the vessel centreline on the x-axis [deg]
γ True wind direction relative to the vessel centreline on the x-axis [deg]
Δ Displacement [t]
ε Factor of atmospheric stability and surface roughness [-]
θ Heeling angle [deg]
θ_d Derived heeling angle used in REG criteria [deg]
θ_D Dynamic heel angle [deg]
θ_f Downflooding angle [deg]
θ_G Gust wind heel angle [deg]
$\theta_{\overline{GZ}\max}$ Heel angle at which $\overline{GZ}$ is maximum [deg]
θ_S Steady heel angle [deg]
θ_v Angle of vanishing stability [deg]
λ Wind heeling lever in BV criteria [m]
ρ_a Air density [kg m^{-3}]

ABS American Bureau of Shipping
BV Bureau Veritas
CE Centre of Effort
CLR Centre of Lateral Resistance
DNV Det Norske Veritas
G Centre of Gravity
IMO International Maritime Organization
IS Intact Stability
KR Korean Register
LR Lloyd's Register
M Metacentre
n.d. No date
NK Nippon Kaiji Kyokai
PC Point of Contraflexure

REG Red Ensign Group
RINA Registro Italiano Navale
US United States
USCG United States Coast Guard
W WAPS
WAPS Wind-Assisted Propulsion Systems
Y Yacht

1. INTRODUCTION

Wind-Assisted Propulsion Systems (WAPS) for ships are on the rise and both system size and the orderbooks of suppliers are growing (DNV, 2024). Most installations are aiming at average energy savings of up to about 20 percent but there are a number of projects with higher ambitions, striving for more than 50 percent savings (DNV, 2024; EMSA, 2023; IWSA, 2024). This requires larger wind propulsion systems with high performance capabilities. To exploit the full potential of wind propulsion and simultaneously warrant safe and efficient ship operation the typical stability risks associated with sail technology need to be reassessed for modern ship and system design. This need is underscored by several high-profile incidents in recent decades in which sailing vessels capsized despite complying with established stability standards (BEA MER, 2025; MAIB, 2025; NTSB US, 1987; TSB Canada, 2011); a recent example is the case of Sailing Yacht Bayesian (MAIB, 2025).

The 2008 Intact Stability Code (IS-Code) from the International Maritime Organization (IMO) stipulates minimum stability criteria for conventional merchant vessels, with classification societies responsible for verifying a vessel's compliance across a range of standard operational and stability conditions. Its origins trace back to the late 19th century (Kobylinski & Kastner, 2003), which coincided with the decline of commercial sailing vessels (Middendorf, 1903), providing an explanation for the omission of the effect of sails on vessel stability in the IS-Code. Nowadays a number of classification societies do impose additional stability criteria for WAPS-equipped vessels. Nonetheless, multiple maritime industry stakeholders recognise that stability is a critical factor for WAPS-equipped merchant vessels but that current intact stability criteria are not necessarily applicable to modern WAPS installations and that a harmonised regulatory framework is lacking (BV, 2024b; DNV, 2024; EMSA, 2023; IWSA, 2024).

There have been a number of studies on the stability of sailing vessels equipped with conventional systems (e.g., (Boer, 2023; Cleary et al., 1996; Deakin, 1988, 1990a, 1990b, 2009). Only a few are known to have examined this for merchant vessels, especially when equipped with modern WAPS. Those that do generally predate the current additional stability criteria (Hu et al., 2015; Kramme, 2014) or address the subject only superficially in passing (Hussain & Amin, 2021; Mohamed Nadzri & Ahmed, 2021). This motivated the undertaking of a master's thesis with the aim to evaluate both the existing additional WAPS stability criteria and the associated operational stability risks. To achieve this objective the criteria were analysed and compared to assess the impact of the gaps and the differences between them. The focus here was on two key areas, the wind acting on the vessel and, the stability response of the vessel to this wind. In addition, it was considered which stability related operational safety risks exist for the various WAPS and how they are addressed in the existing criteria.

In total 15 different stability standards were selected, based partly on the size of the respective classification societies (Lloyd's list, 2023). If stability criteria were available for both sailing yachts and WAPS both were included to ensure comprehensive coverage as it was observed that sailing yacht criteria have often served as the foundation of the stability criteria for WAPS vessels. In the case of the Red Ensign Group (REG) sailing yacht criteria, only part B, which incorporates elements from part A, is considered. The Indian Register of Shipping and the Polish Register of Shipping are excluded as they do not provide additional WAPS stability criteria. Similarly, the China Classification Society was excluded as its additional criteria apply solely to Flettner rotor sail installations and

portray only minor variations compared to other stability standards. The thesis also incorporated two sets of naval stability criteria on account off their distinct approach compared to merchant vessel criteria in assessing stability under wind, for brevity they are excluded from this paper.

The stability criteria analysis incorporated WAPS installations of varying dimensions and types to ensure relevance to real-world applications. Due to variability in manufacturer specifications and limited data availability, reasonable assumptions regarding system dimensions were made. The Indorig and Dynarig systems represent conventional WAPS of the wing sail variety with distinct operational characteristics. Flettner rotors and suction sails represent modern mechanical systems which rely on a constant active power input to function but also possess differences in the physical and operational characteristics.

The thesis was done within the framework of the Rasant project developing conceptual designs for modern sail cargo vessels based on design tools for the optimisation of important performance and safety parameters. This paper presents an excerpt of the thesis work and is organised as follows. Section 2 introduces the effect of wind on a vessel's stability and the various WAPS considered in the thesis. Section 3 subsequently addresses the various stability standards considered in this study as well as a concise comparison of the different criteria, including the various calculation methods and assumptions. Operational stability risks which may require additional attention and guidance are covered in section 4. Finally, the discussion and conclusion on the key takeaways and proposals for future requirements are mentioned in section 5 and section 6.

2. WIND AND STABILITY

2.1 Lateral Aerodynamic Loads

The apparent wind acting on a vessel is the vector sum of the true wind vector, with velocity V_T and relative direction γ, and the vessel speed vector V_S, constructed as illustrated in Figure 1. When exposed to this apparent wind with velocity V_A and relative direction β a sail (i.e., the WAPS) generates perpendicular lift F_L and parallel drag F_D forces, resulting in a force F_Y acting laterally to the vessel in the Y-direction. For a WAPS with a fixed wind area A, F_Y is primarily influenced by β, V_A, and the magnitude of the lift C_L, drag C_D and lateral C_Y aerodynamic force coefficients,

$$F_Y = 0.5\rho_a V_A^2 A(C_L \cos\beta + C_D \sin\beta) = 0.5\rho_a V_A^2 A C_Y = PA, \quad (1)$$

where ρ_a is the air density and P is the wind pressure (Marchaj, 1979). The WAPS's F_Y is generally assumed to act at the Centre of Effort (CE), which is often taken as the area centroid.

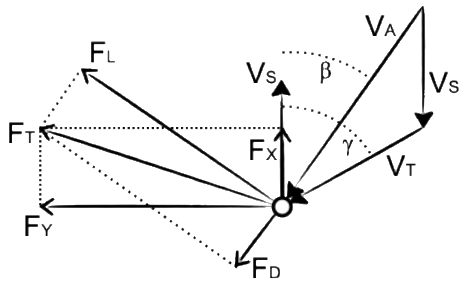

Figure 1. Diagram illustrating the connection between the true wind and apparent wind as well as the aerodynamic force components created by the apparent wind acting on a WAPS.

The basic equation for F_Y as depicted above is assumed to be consistent across the various stability standards. However, aside from ρ_a, where deviations are considered negligible, significant variations and gaps were observed in other variables of the equation, affecting the outcome. These are addressed in section 3.

2.2 Wind Assisted Propulsion Systems

The WAPS were separated in the two categories illustrated in Figure 2 based on their physical characteristics. The effects of aerodynamic interaction between multiple WAPS on the magnitude of the aerodynamic forces (Marchaj, 1979), was generally disregarded unless explicitly stated otherwise. Coefficient data for conventional passive systems, which do not require an active energy input to generate lift, were obtained from Schenzle (1985a) for the Indorig and from Wagner (1967) and Bordogna et al. (2016) for the Dynarig. In contrast to the conventional systems, mechanical WAPS such as Flettner rotors and suctions sails require an active external energy input to generate aerodynamic lift. Their coefficient values were taken from Kisjes (2017) and Malavard (1984) for the suction sail, and from Vahs (2020) for the Flettner rotor.

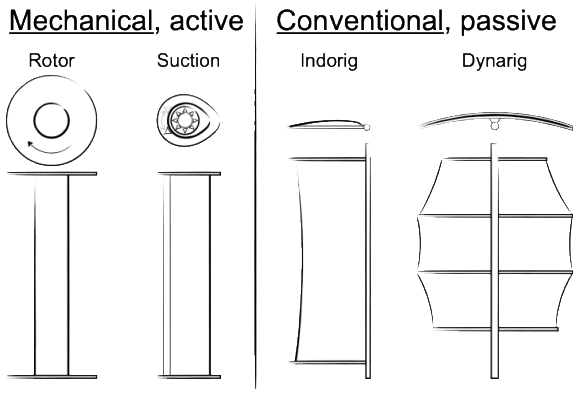

Figure 2. Simplified illustrations of the different types of WAPS where the mechanical systems require an active energy input to generate aerodynamic lift and the conventional ones do not.

Flettner rotors' functionality is based on the Magnus effect (1853), where a spinning cylinder generates a lift force perpendicular to rotational axis and the wind direction (Swanson, 1961) and first applied for ocean-going merchant vessels in the 1920's (Borg, 1986; Flettner, 1928). With a fixed rotor size, the speed ratio S_R (the rotor's tangential velocity relative to V_A) is a key element influencing aerodynamic coefficient magnitude; the system size was assumed irrelevant for a fixed A_R (Aspect Ratio). The rotors rely on electric power to spin (Eco Flettner, 2024) and the specifications of four different rotor sizes with a constant A_R were based on commercially available systems (Anemoi, 2024; Eco Flettner, 2024; Farwind Energy, 2024; LR, n.d.; Norsepower, 2024).

Suction sails follow a different operating principle, with an ovaloid shaped wing form and end-mounted electric axial fans to induce boundary layer suction at the trailing edge to enhance boundary layer flow attachment, as well as a movable trailing flap, achieving higher C_L values compared to conventional systems (Kisjes, 2017). They were developed as an alternative to the Flettner rotor by Malavard (1984) and the Cousteau society (Charrier et al., 1985; Cousteau et al., 1984). Another version, not considered here and marketed as the Ventofoil by Econowind (n.d.), employs a symmetrical teardrop-shaped cross-section with axial fans mounted on the centre plane and without flap. The study considered two system sizes of 16 and 32 meters high with the same constant A_R. In addition to the fixed projected sail area A, sail shape and A_R, the aerodynamic coefficient values and F_Y can be manipulated by changing the sail's angle of attack α and the suction coefficient C_q,

$$C_q = \frac{Q}{AV_A}, \tag{2}$$

where Q is the volumetric suction flow produced by the electric fans.

The Indorig and Dynarig, developed in the second half of the 20th century (Schenzle, 1985b; Wagner, 1967), are modern adaptations of the fore-and-aft and square rigs with comparable physical characteristics and are also assumed to reasonable represent fixed wing systems. With a fixed sail shape the magnitude of C_L and C_D varies based on α; F_Y can be lowered further by reducing sail area (i.e., reefing). In that case the CE height of the Dynarig will decrease, as it is reefed vertically, and the CE of the Indorig, which is reefed horizontally, will remain at the same vertical location. The data sets from Wagner (1967) and Schenzle (1985a) were not corrected for the effect of the model hull on the aerodynamic coefficient values. Wagner considered this to be insignificant and for simplicity this assumption was extended to this study and coefficient values were not corrected.

2.3 The Wind Heeling Moment and the Opposing Righting Moment

The wind heeling moment M_H, illustrated in Figure 3, is typically calculated as,

$$M_H = F_Y Z = 0.5\rho_a V_A^2 C_Y A Z = PAZ, \tag{3}$$

where Z is upright heeling arm between the CE and the Centre of Lateral Resistance (CLR), which is often assumed to be located at mid draft T (see Figure 3).

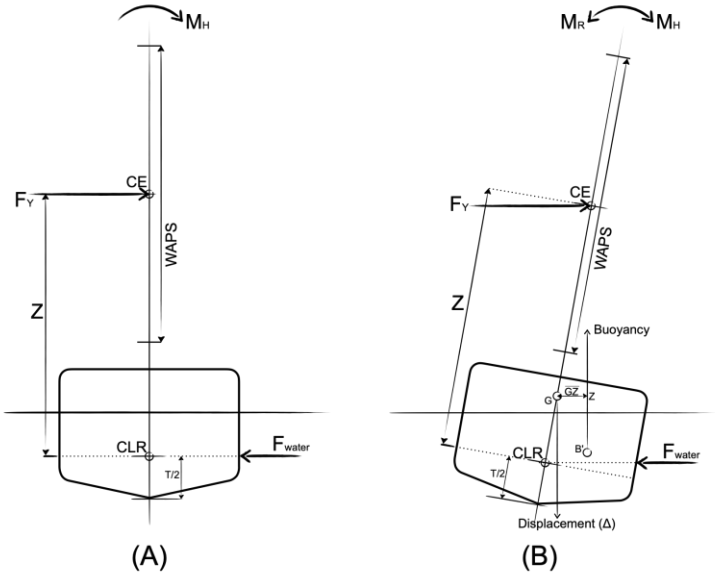

Figure 3. Illustration of F_Y and the opposing hydrodynamic force F_{water} acting on a vessel, as well as the other variables which determine the magnitude of M_H and M_R in upright (A) and inclined (B) condition.

The stability response of the vessel to M_H depends primarily on the magnitude of the counteracting righting moment M_R,

$$M_R = \overline{GZ}\Delta, \tag{4}$$

where $\overline{GZ}$ is the righting lever and Δ the vessel's displacement. Here notable inconsistencies were also encountered across the different stability standards in relation to, among others, Z, the M_H equation format, and how M_H is assumed to change with an increase in heel. These potentially pose a risk factor as they affect the magnitude of M_H.

2.4 Assessing a Vessel's Stability

Plotting M_R or $\overline{GZ}$ against the heeling angle θ returns the stability curve, illustrated in Figure 4. This graph provides insight on the maximum M_R and $\overline{GZ}$, the point of contraflexure (PC) at which the deck edge submerges and the angle of vanishing stability θ_v up to which $M_R > 0$ and the vessel will theoretically return to its initial position if M_H decreases. The initial metacentric height $\overline{GM_0}$ is the upright distance between the vessel's centre of gravity (G) and the metacentre (M), located at the intersection of the buoyancy force line and the centreline. It serves as a measure of the stability at low inclination angles.

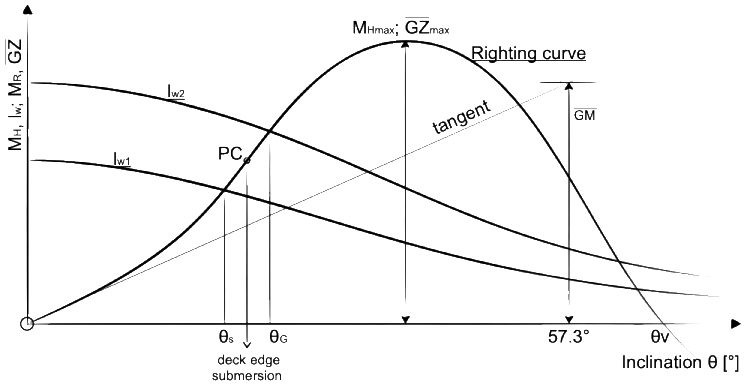

Figure 4. Wind heeling lever curve overlayed on righting lever curve.

Figure 4 further illustrates how the curves of both M_H and the steady wind heeling lever l_{w1},

$$l_{w1} = M_H/\Delta\,, \tag{5}$$

can be superimposed on the stability curve. In this steady wind the vessel is assumed to heel up to steady heel angle θ_S where $M_H = M_R$. In gusts the steady wind velocity temporarily increases to a maximum gust wind velocity. A vessel's ability to withstand this transient load of a dynamic nature is a critical aspect of its stability. M_H may increase significantly, resulting in the gust wind heeling lever l_{w2}. The increase is generally described with the gust factor G_f. However, the actual increase depends heavily on the physical characteristics of the WAPS in question. The intersection between l_{w2} and the stability curve is marked here with the gust wind heeling angle θ_G, but a vessel is often assumed to develop additional dynamic heel due to the presumed kinetic energy of the sudden wind gust.

2.5 Dynamic Stability

In a gust, the vessel's heel is often assumed to exceed the equilibrium angle θ_G, where the gust M_H equals M_R (see Figure 4). As an event of dynamic nature, a gust introduces kinetic energy, causing the vessel to continue heeling until it reaches the dynamic heeling angle θ_D, at which point all the heeling energy has been spent and absorbed by the righting energy. Figure 5 (A) illustrates this for a scenario in which the gust is encountered in the upright position, for example following a windward roll induced by wave action. Figure 5 (B) illustrates the response when the gust is encountered at θ_S. Provided the vessel's stability is sufficient to absorb the additional energy, it will return to its original steady heel angle once the gust subsides.

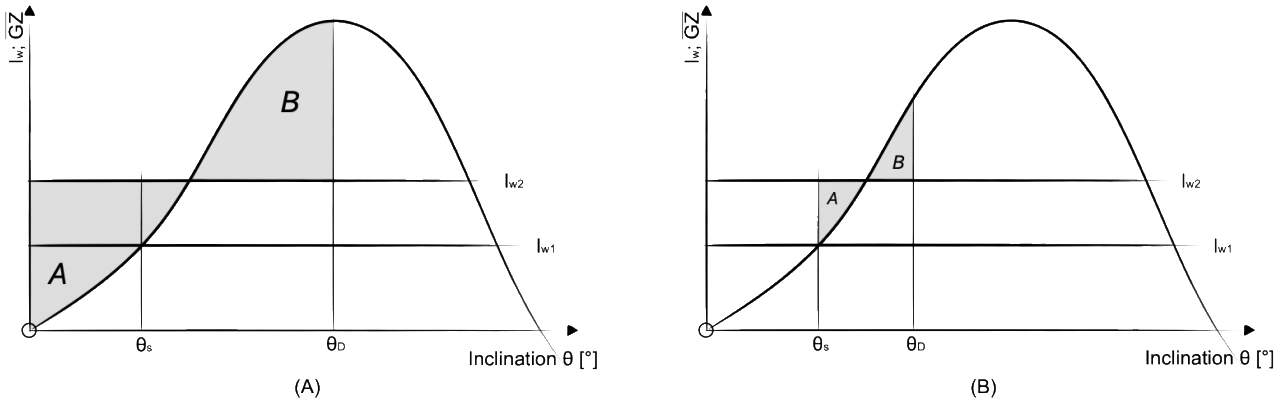

Figure 5. Illustrating the effect of a gust encountered when the vessel is rolled to windward (A), and when the vessel is sailing at a steady heeling angle (B).

The dynamic heel angle is influenced by the characteristics of both the WAPS and the vessel. Although Figure 5 and the IMO (2008a) criteria assume that θ_D is reached when an energy balance exists and area 'A' equals area 'B' this is not always the case. While most stability criteria apply this energy balance method in some form to ensure adequate dynamic stability, the damping effects of wind on the WAPS and underwater appendages can significantly influence the vessel's response. These effects may reduce θ_D considerably, potentially limiting it to only a small margin beyond θ_G (Deakin, 1990a).

3. COMPARING ADDITIONAL STABILITY CRITERIA

This section will discuss both the manner in which M_H is calculated in stability standards as well as the stability criteria which govern the vessel's stability response. The criteria in the IS-Code, which all merchant vessels must comply with, serve as a baseline. The scope of the classification societies whose stability criteria were reviewed is summarised in Table 1 with the Naval criteria and RINA's (Registro Italiano Navale's) yacht criteria, which match those from the REG, omitted for brevity.

Table 1. Overview of the classification societies whose stability standards containing additional stability criteria for WAPS (W) or for Yachts (Y) were covered.

Criteria	IMO	NK	KR	LR	ABS	DNV	BV	RINA	REG	USCG
W	–	X	X	X	X	X	X	X	–	–
Y	–	–	–	–	–	X	X	–	X	X

The majority of the additional criteria strongly resemble the IS-Code, in which cases it is assumed to have served as their foundation. Existing sailing yacht stability criteria served as the basis in the case of Det Norske Veritas (DNV, 2021, 2025a), drawing on legacy criteria from the Germanischer Lloyd (GL), and Bureau Veritas (BV, 2024a, 2025). Other stability criteria considered were those from Nippon Kaiji Kyokai (NK, 2024), Korean Register (KR, 2025), Lloyd's Register (LR, 2025), American Bureau of Shipping (ABS, 2022), RINA (2025), REG (2024), and the United States Coast Guard (USCG, n.d.-b). A harmonised framework across the various stability standards is absent for both WAPS-equipped vessels and sailing yachts and inconsistencies were also encountered in the underlying assumptions when calculating M_H.

3.1 Determination of the Wind Heeling Moment Acting on the Vessel

3.1.1 Wind velocity

As illustrated in Table 2, compliance across a range of wind velocities is not uniformly explicitly accounted for. Instead, some criteria refer to a single wind velocity, in line with the IS-Code, which does not align with the practical operation of WAPS. This may unnecessarily limit system size, reducing operational efficiency. It is unclear if this is really applied in practice, considering that KR does not explicitly allow it but it was considered for the sailing vessel Juren Ae, classed under KR (Kostec, 2024).

Table 2. Wind velocity considerations in the various stability criteria.

Criteria		IMO	NK	KR	LR	ABS	DNV		BV		RINA	REG	USCG
							W	Y	W	Y			
Range	Ship + WAPS, 26 m s^{-1}	X	X										
	Ship, 26 m s^{-1}; WAPS, varies										X		
	Ship + WAPS, varies				X		X	X	X	X	X	X	X
	Not Clear			X		X							
Wind reference	True wind, 2008 IS-Code	X	X	X							X		
	True wind lateral							X					
	Apparent wind											X	
	Not Clear				X	X	X		X	X			X

The difference between true and apparent wind is also often neglected and most criteria appear to either assume a true lateral wind or lack clarity regarding which wind reference should be applied in the calculation of M_H. Figure 6 illustrates that, depending on γ and V_S there are notable differences between V_A and V_T, and considering that these are squared in the F_Y equation the effect can be significant. If this distinction is disregarded in practice or when determining operational limits, F_Y and M_H may be higher than anticipated. It is therefore essential to specify clearly on which wind reference the operational limits are based and if true wind is used corresponding V_S limits should also be considered. The potential adverse effects can be mitigated with effective WAPS depowering in conjunction with operating limits such as heeling angle. In certain cases, additional uncertainty is introduced by referencing apparent wind for design loads while omitting it in the stability criteria; a uniform approach in this regard would be beneficial.

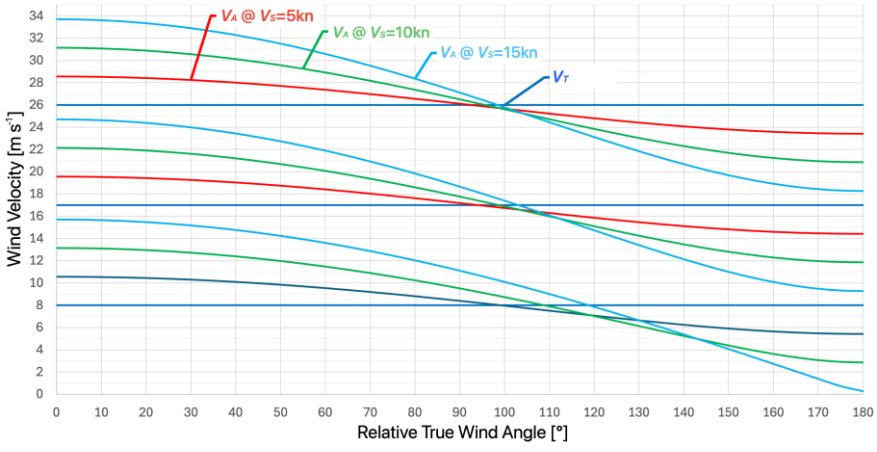

Figure 6. Graph demonstrating how for a fixed V_T a change in V_S up to 15 knots affects the magnitude of V_A at varying γ ranging from 0° up to 180°.

3.1.2 Wind Gradient

The wind gradient describes the increase of wind velocity with height above the water surface and can be approximated in the form of the wind profile power law (Hsu, 1988),

$$V_z = V_{\mathrm{ref}} \left(\frac{z}{z_{\mathrm{ref}}} \right)^{\varepsilon}, \tag{6}$$

where V_z is the wind velocity at a height z above the water surface and V_{ref} is the reference wind velocity at height z_{ref}, often 10 meters (ABS, 2005). The factor ε is a measure for atmospheric stability and surface roughness, a value of 0.10-0.11 is considered appropriate at sea (Hsu et al., 1994; Hsu, 1988; Kobylinski & Kastner, 2003). As summarised in Table 3 this approach is not widely adopted, although LR (2025) does apply $\varepsilon = \frac{1}{9} \approx 0.11$. BV (2025) does not consider the wind profile power law, instead using the wind pressure height coefficient C_H, as applied by the USCG and the IMO for Mobile Offshore Drilling Unit criteria (IMO, 2008a; USCG, n.d.-a).

Table 3. Wind gradient consideration in the various stability criteria.

Criteria		IMO	NK	KR	LR	ABS	DNV W	DNV Y	BV W	BV Y	RINA	REG	USCG
Wind gradient	Uniform	X	X	X							X		
	$V_z = V_{10} \cdot (\frac{z}{10})^{\frac{1}{9}}$				X								
	$V_z = V_{15.3} \cdot (\frac{z}{15.3})^{\frac{1}{7}}$					X							
	Coefficient C_H								X				
	Not Clear						X	X		X		X	X

Figure 7 demonstrates that the differences between wind gradient methodologies will be more pronounced at greater heights. The increased wind velocity and wind load on the upper parts of the WAPS means that the wind gradient may also increase Z by raising the location of the CE, as was also discussed by Deakin (1988).

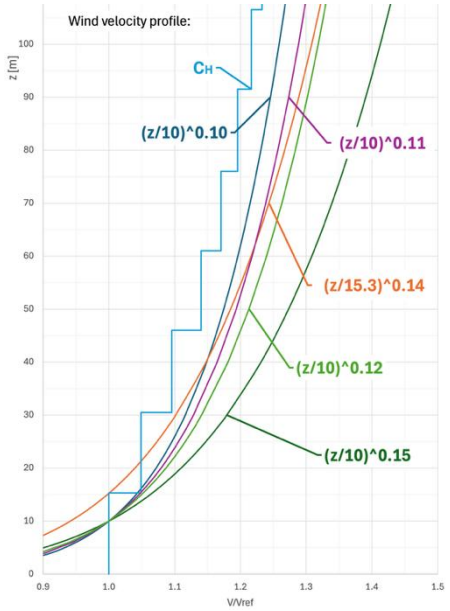

Figure 7. The various wind velocity profiles applied in criteria for $V_{10} = 1\ \mathrm{m\ s^{-1}}$ with C_H corrected to wind velocity instead of wind pressure.

In addition to the limited number of stability criteria considering some form of wind gradient, further ambiguity is introduced when the design-load and stability methodologies do not correspond. Variations or omittance of the wind gradient may result in an underestimation of M_H, particularly for larger WAPS. Its effective impact is up for debate though as it largely disappears during gusts and squalls that pose a threat in terms of stability (Wolfson Unit, 2006) and the operation of conventional sailing vessels is generally not determined by the calculated predicted M_H (Deakin, 2009). However, this assumption does not necessarily extend to automated systems where the predicted values play a larger role and could potentially affect the accuracy of operational limits. Adverse consequences could be mitigated through 'active' (automated) sailing based on actual wind velocity measurements and through the use of additional operational limits such as steady heel instead of theoretically predicted heeling moments. The WAPS type and effectiveness of its depowering methods could further reduce the risk.

3.1.3 Gust Factor

The value of 1.5 as a gust factor G_f to describe the increase in P, used in the IS-Code and based on Watanabe et al. (1956) accounts for the mitigating effects of rolling motions and reduction in relative wind velocity due to the vessel's lateral drift speed. Table 4 illustrates that it has been adopted by several criteria in which case it is generally applied to l_{w1} to calculate l_{w2}.

$$l_{w2} = G_f l_{w1}, \tag{7}$$

Its suitability for WAPS remains uncertain as it is based on conventional motor vessels. Given that WAPS-equipped vessels may exhibit different roll and drift behaviour due to the damping or excitation effect of the wind propulsion systems and additional underwater appendages, the associated mitigating effects may be less pronounced, and the higher gust factors could be more appropriate. The rationale for higher gust factors is supported by Kobylinski and Kastner (2003) and Deakin (1991), especially because it can be significantly higher in squalls (Deakin, 2009).

Table 4. Gust factor consideration in the various stability criteria.

Criteria		IMO	NK	KR	LR	ABS	DNV		BV		RINA	REG	USCG
							W	Y	W	Y			
Gust factor	$G_f = 1.5 \cdot P$	X	X	X	X	X					X		
	$G_f = 2.25 \cdot P$						X						
	$G_f = 2.0 \cdot P$											X	
	–							X					X
	Not Clear								X	X			

In a few cases there is some ambiguity regarding gusts. BV (2025) WAPS criteria do not apply a gust factor but instead specify that the maximum wind velocity including gusts is to be used, making it unclear how steady wind velocity limits should be determined. In contrast, BV (2024a) yacht criteria appear to suggest that the maximum steady wind velocity should be applied, creating further uncertainty. DNV (2021) yacht criteria do not address gusts either, but based on WAPS-vessels to which these rules were applied gusts are accounted for by the 40% energy balance margin, resembling United States (US) naval criteria (Sarchin & Goldberg, 1962). However, DNV (2025a) WAPS criteria continue to apply this 40% margin in conjunction with an additional gust factor. This suggests that gusts are effectively twice accounted for, although this may be reasonable considering that according to Lee (2019) the US its 40% margin was criticised for its arbitrary and unclear origins.

The response of WAPS to a gust may vary depending on the system's characteristics and operational behaviour, affecting the actual increase of M_H and associated risk on stability, as addressed in section 4.1. Furthermore, the impact of applying the gust factor to the true wind, as

done in the IS-Code, or to the apparent wind, as done by the REG (2024), is an aspect which for simplicity was omitted in this study but warrants further exploration and clarification.

3.1.4 Lateral Force Coefficient

Irrespective of the WAPS type, its C_Y may vary considerably with β, as demonstrated in Table 5 this is not universally considered. The IS-Code's methodology and the criteria which explicitly replicate it consider a lateral true wind where $C_Y = C_D$ and dismiss this completely. And although a number of stability criteria specify that the relative wind direction for the maximum C_Y should be considered, explicit clarity on the expectations is often lacking. Particularly if the maximum total C_Y does not occur in beam winds this may result in a significant underestimation of the total M_H. The relative contribution of both hull and WAPS also is an important factor to consider here as their respective maximum C_Y may not occur at the same β, affecting the total C_Y. A simplifying measure in this regard would be to consider the hull C_Y fixed, even though this is seldom the case and it will generally decrease sharply when $\beta < 60°$ (Blendermann, 1986, 1993). While this may be too conservative an approach for situations where the largest WAPS C_Y occurs at $\beta < 60°$ it would not present a safety risk and correspond reasonably well for the conventional WAPS which reach their max. C_Y at $\beta \approx 60°$ (Schenzle, 1985a; Wagner, 1967).

Table 5. Lateral force coefficient consideration in the various stability criteria.

Criteria		IMO	NK	KR	LR	ABS	DNV		BV		RINA	REG	USCG
							W	Y	W	Y			
C_Y	Beam wind $C_Y = C_D$	X		X									
	Max. C_Y				X		X					X	
	Not Clear		X			X		X	X	X	X		X

A further consideration is that, depending on the WAPS type, C_Y may reduce with an increase in wind velocity such as during gusts. This is primarily the case for mechanical systems, in particular for Flettner rotors, as will be addressed in section 4.1.

3.1.5 Wind Area

Overlapped wind areas are not included in IS-Code, which defines the wind area as the 'projected lateral area of the exposed ship and cargo above the waterline' (IMO, 2008a). In a number of cases(see Table 6) this approach is explicitly adopted or implied through reference to the projected or profile area. However, in particular for cases where the highest C_Y does not occur under beam wind conditions, no conclusive evidence was found to support the omission of overlapped windage areas. While it may be (partially) valid under specific conditions the potential for underestimating the effective windage area requires a cautious approach. Given the significant impact that underestimating the effective area would have on the wind heeling moment, it may be more prudent to always consider the total area, including overlapped sections.

Table 6. Wind area consideration in the various stability criteria.

Criteria		IMO	NK	KR	LR	ABS	DNV		BV		RINA	REG	USCG
							W	Y	W	Y			
Wind area	Lateral profile	X		X						X			X
	Lateral sectional								X				
	Total sectional				X								
	Total		X			X	X	X			X	X	

3.1.6 Heeling Arm

The simplification that the heeling arm is the distance between the CLR, generally assumed at mid-draught, and the wind area centroid is the approach applied in the IS-Code and commonly reciprocated (see Table 7). However, as Okada (1952) demonstrated, this assumption is not always valid and the actual wind pressure centre may be located significantly higher than the wind area centroid. Okada attributed this effect in part to the influence of the wind gradient, an observation supported by, inter alia, Deakin (1990a). To allow the simplifying measure of using the wind area centroid as the CE for Z, the IS-Code follows the methodology from Sato et al. (1954) who suggested this solution, provided that the lateral C_D is increased to compensate for the vertical difference between the wind area centroid and the actual CE.

Table 7. Heeling arm consideration in the various stability criteria.

Criteria		IMO	NK	KR	LR	ABS	DNV		BV		RINA	REG	USCG
							W	Y	W	Y			
Heeling Arm $\boldsymbol{Z}$	CLR – Wind area centroid	X	X	X	X	X	X	X	X	X	X	X	X

The IS-Code assumes that the actual wind pressure centre is 20% higher than the wind area centroid (IMO, 2008a). This is illustrated in Figure 8 where H is the actual heeling arm, from the CLR at mid-draft up to the wind pressure centre, and H_0 is the distance up to the wind area centroid. The ratio of H to H_0 is therefore 1.2, i.e., $(H/H_0) \approx 1.2$. To compensate for this when calculating M_H the lateral C_D is multiplied by (H/H_0) so that $C_D\,(H/H_0) \approx 1.22$, which is the value used to calculate the wind pressure value of 504Pa, calculated using Eq.8 for $\rho_a = 1.222$ and $V_A = 26$. Consequently, it can be deduced that $C_D \approx \frac{1.22}{(H/H_0)} \approx \frac{1.22}{1.2} \approx 1.017$. However, the standard equation to calculate M_H, see Eq.3, would suggest that $C_D \approx 1.22$.

$$P = 0.5\rho_a V_A^2 C_D\,(H/H_0) \tag{8}$$

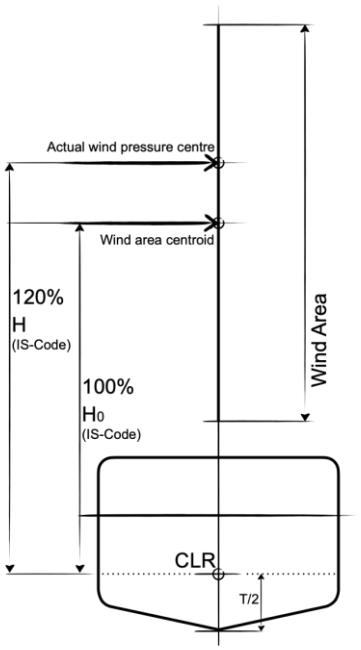

Figure 8. Visual representation of the IS-Code's assumed vertical disparity between the wind area centroid and the actual wind pressure centre.

When the IS-Code criteria and methodology are applied to WAPS-equipped vessels, as done by, for example, KR (2025), care should be taken that the value of 1.22 cannot simply be substituted by a different C_Y value. This may disregard (H/H_0), potentially resulting in an underestimation of M_H. Table 8 illustrates, with an example, the effect of disregarding this vertical disparity between the actual CE and the wind area centroid for a WAPS-equipped vessel with $C_Y = 1.30$. In this instance not taking the IS-Code's factor of $C_D\ (H/H_0) \approx 1.22$ would underestimate P, and thus M_H by ±17%.

Table 8. The effect of dismissing the assumed vertical disparity between the wind pressure centre and the wind area centroid when applying the IS-Code criteria to WAPS-equipped vessels.

	C_Y [-]	(H/H_0) [-]	$C_Y(H/H_0)$ [-]	P [Pa]	% change
IS-Code	1.02	1.2	1.22	504	
Substituting $C_Y = 1.02$ with $C_Y = 1.30$	1.30	1.2	1.56	644	+28%
Substituting $C_Y(H/H_0) = 1.22$ with $C_Y = 1.30$ while dismissing (H/H_0)	1.30		1.30	537	-17%

RINA (2025) incorporates an additional factor of $\frac{C_D \cdot Z_w}{Z_0} \leq 1.22$ in the equation for l_{w1}, where Z_w is the heeling arm and Z_0 is the vertical distance between the wind area centroid and a point at mid-draft. Although its intention is unclear, this suggests that RINA considered the same approach. It may however be unnecessarily conservative as the equation applies a fixed hull P of 504 Pascal (0.0514 t) which already includes $C_D\ (H/H_0) \approx 1.22$ (IMO, 2008a), raising doubts on its intended application.

Dividing the WAPS area into multiple layers with their own Z, for which M_H is calculated separately, in combination with the wind gradient, as applied by LR (2025), largely avoids this issue as it accounts for both the increase in wind velocity with height and the effect of the wind gradient on the CE. Even though each layer's CE location is still assumed to be at the area centroid this inaccuracy is of minimal effect. A potentially escalating factor is the rise of the CE with vessel inclination if WAPS are mounted off-centre. This was not covered in the thesis, and its effect could be explored further. Furthermore, it should be considered that if a single Z is used when calculating the wind heeling moment the effect of variations in WAPS A or C_Y, for example due to reefing or depowering, should be accounted for in the magnitude of Z.

3.1.7 Wind Heeling Moment Variation with Vessel Inclination

Table 9 demonstrates how there is no uniform approach across the stability criteria regarding the assumed the variation of M_H with an increase in θ. inclination. The impact of the various M_H variation factors on the initial upright M_H is illustrated in Figure 9. The straightforward assumption that it remains constant, as applied in for example the IS-Code (IMO, 2008a), adds an additional margin of safety (Kobylinski & Kastner, 2003) and is considered reasonable for large merchant vessels (Luquet et al., 2015), whose projected lateral area changes little within the relevant inclination range. However, there is no substantive evidence that supports the extension of this assumption to the WAPS's M_H, which is often found to decline with heel.

Table 9. Wind heeling moment variation with inclination in the various stability criteria.

Criteria		IMO	NK	KR	LR	ABS	DNV		BV		RINA	REG	USCG
							W	Y	W	Y			
Variation	Constant	X	X	X	X	X					X		
	Varies						X	X					
	$\cos^{1.3}\theta$								X			X	
	$\cos^{2}\theta$									X			X

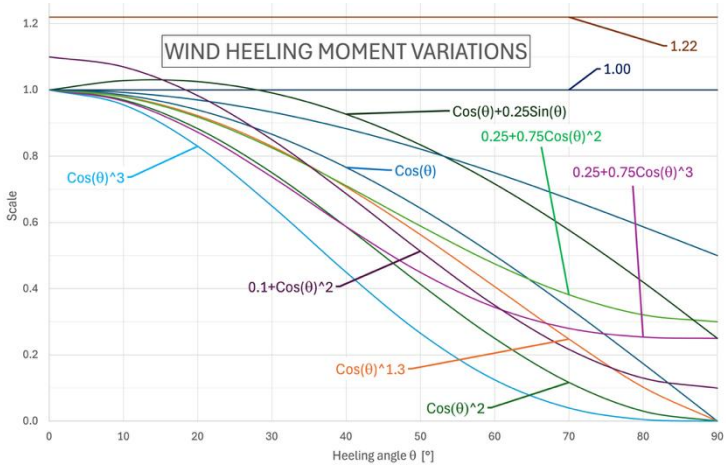

Figure 9. Wind-heeling lever variations.

The rationale behind the various alternative methodologies applied in stability criteria is well-documented but uncertainties remain regarding their accuracy and applicability to all WAPS, in particular because they are often based on vessels without WAPS or equipped with conventional systems. This reflects in the operational envelope, although inaccuracies can be mitigated through effective depowering. If a single M_H covering both WAPS and hull is applied, consideration of a residual heeling moment at 90° heel may be necessary, owing to the exposed wind area of the inclined hull, although this varies with vessel proportions and conventional sailing vessels and Deakin (1990a) found it to be negligible compared to the initial upright M_H.

DNV does not specify a variation, but vessels classed under DNV(GL) have been found to apply, among others, $0.25 + 0.75\cos^3\theta$ (SDC, 2021), which is based on conventional vessels (Wendel, 1959) and $\cos^2\theta$ (SDC, 2010). The reduction with $\cos^2\theta$ (Middendorf, 1903) assumes that sails behave as a flat plate in beam winds (Deakin, 1990a). Deakin (1990a) found the more conservative factor of $\cos^{1.3}\theta$ to better fit the behaviour of conventional sailing vessels. As lift acts perpendicular to a sail's vertical axis (Larsson et al., 2022) the reduction of WAPS with higher C_L values at low β, such as Flettner rotors, could be even less pronounced. In such cases the application of the effective apparent wind angle method, described by Larsson et al. (2022), could perhaps be explored as an alternative to the variation factor, in which case it would have to be considered if the benefits outweigh any additional complexity.

The impact of differences in variation factors on θ_S was found to be relatively minor as it does not significantly alter the wind heeling moment at low inclination angles. Their influence on dynamic stability was found to more significant, particularly for vessels with high down-flooding angles.

A simplifying measure could be to separate the M_H contributions of the hull and the WAPS. This allows the hull M_H to be constant, consistent with the IS-Code, while the WAPS M_H is added separately with a suitable variation factor without having to consider a residual heeling moment at 90° heel. This could facilitate compliance with stability criteria, particularly in cases where a WAPS is retrofitted and specific data on a combined C_Y and accurate Z is unavailable.

3.1.8 Wind Heeling Moment Equation Format

Further inconsistencies beyond those previously discussed may be introduced depending on the formulation of the final M_H equation, where, as illustrated in Table 10, even when disregarding the variety in symbol notations for the wind heeling moment lever a uniform approach regarding the equation format is absent. An example is the summation of the WAPS wind pressure and hull wind pressure, along with a single A and a single Z, as applied by RINA (2025), which overlooks the relative contributions of the hull and WAPS. Figure 10 demonstrates that this may result in

significantly higher results compared to a method which treats the WAPS M_H and hull M_H completely separately (NK, 2024), even without considering RINA's additional factor $\frac{C_D \cdot Z_W}{Z_0}$, introducing the potential for significant discrepancies.

Table 10. Wind heeling lever equation formats as considered in various stability criteria.

Criteria		IMO	NK	KR	LR	ABS	DNV W	DNV Y	BV W	BV Y	RINA	REG	USCG
Equation	$l_{w1} = \frac{P \cdot A \cdot Z}{1000 \cdot g \cdot \Delta}$	X		X		X							
	$l_{w1} = \frac{0.0514 \cdot A \cdot Z}{\Delta} + \frac{F \cdot Z}{1000 \cdot g \cdot \Delta}$		X										
	$l_{w1} = \frac{M_S + M_W}{\Delta}$				X								
	Varies						X	X					
	$\lambda = \frac{F \cdot Z}{1000 \cdot g \cdot \Delta} \cdot \cos^{1.3}\theta$								X				
	$\lambda = \frac{F \cdot Z}{9807 \cdot \Delta} \cdot \cos^{2}\theta$									X			
	$l_{w1} = \frac{C_D \cdot Z_W}{Z_0} \cdot \frac{P \cdot A \cdot Z}{1000 \cdot g \cdot \Delta}$										X		
	$HA = \frac{0.5 \cdot \rho \cdot V^2 \cdot (A_{sails} h_{sails} C_{sails} + A_{hull} h_{hull} C_{hull})}{1000 \cdot g \cdot \Delta} \cdot cos^{1.3}\theta$											X	
	$HA \cdot cos^{2}\theta$												X

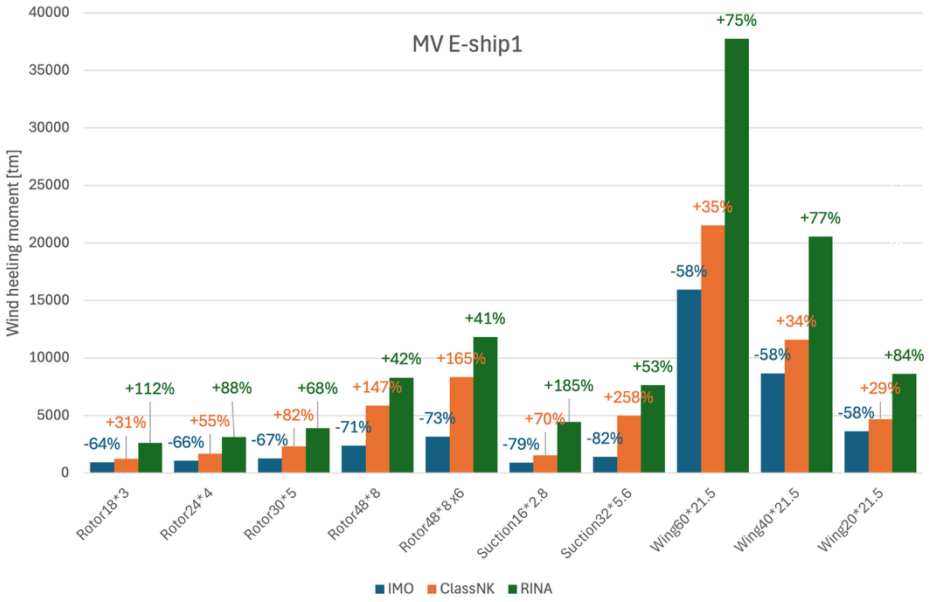

Figure 10. MV *Eship1*, IMO; NK; RINA equations compared for $V_A = 26\ \mathrm{m\ s^{-1}}$ and $\beta = 60°$ → Rotor $C_Y = 1.97$; Suction $C_Y = 4.39$; Wing $C_Y = 1.67$; Hull $C_Y = 1.22$.

When a single wind force and heeling arm are applied in calculation, as is the case with, e.g., the IS-Code, the relative contributions of the WAPS and hull to the overall wind heeling moment are not inherently accounted for. A single combined heeling arm based on the centroid of the total area assumes that both WAPS and hull have the same C_Y. However, in particular if the WAPS generates a significant share of the heeling moment, the actual combined heeling arm may be significantly larger than predicted. Figure 11 demonstrates that for a situation of four large Flettner rotors on the Motor Vessel *EShip1*, the effect of not considering that the WAPS's C_Y is larger than that of the hull could lead to a significant underestimation of Z. At the same time, depowering in this context should then be recognised as a mechanism that decreases M_H by reducing both F_Y and Z.

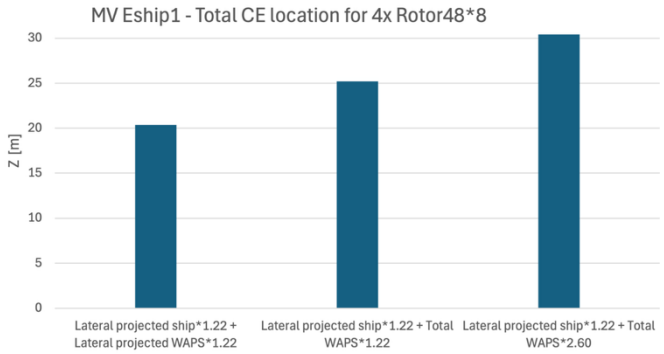

Figure 11. Effect of different calculation methods on the total CE for Eship1 with 4*Rotor$_{48*8}$ and C_Y of 1.22 and 2.60.

3.2 Stability Response of the Vessel to the Wind Heeling Moment

3.2.1 Stability Range

The stability range criteria outlined in Table 11 typically refer to the angle of vanishing stability θ_v, up to which M_R remains positive. This criterion is often applied to sailing yachts. A value of 90°, as used in the REG (2024) criteria, assumes that the positive and negative influences on M_R, whose effects are difficult to predict, largely cancel each other out (Wolfson Unit, 2006). The rationale for the specific lower threshold values of 60° of 70° is unclear and may be based on empirical assessments of existing vessels.

Table 11. Stability range criteria.

Criteria		IMO	NK	KR	LR	ABS	DNV W	DNV Y	BV W	BV Y	RINA	REG	USCG
Stability Range	–	X	X	X	X	X	X		X	X	X		
	≥ 60° without keel							X					
	≥ 90° with keel												
	≥ 90° if Sail Area Displacement ratio >10											X	
	< 90° if Sail Area Displacement ratio <10												
	≥ 70° (partially) protected waters												
	≥ 90° exposed waters												X

A lower stability range is generally considered acceptable for larger vessels as the relative size of breaking waves decreases, reducing the likelihood of a knockdown (MCA, 2004; Oossanen, 1997). However, such an event remains possible, and its severity is not diminished, meaning the associated risk cannot be disregarded (Wolfson Unit, 2006). Watanabe et al. (1956) proposed that if two of the three criteria, dynamic stability, $\overline{GZ}_{\max}$, and θ_v, are met, the third one can be reasonably estimated, and they consequently considered θ_v redundant. The IMO excluded θ_v from its stability criteria due to the wide variation observed in case analyses during the IS-Code development (IMO, 2008b).

It should also be considered that significant heel may result in cargo shifting, which can impose significant additional strain on the vessel's stability. This effect is not accounted for in the fixed stability range of 90° (Deakin, 1990a). Likewise, severe downflooding during prolonged heel can have a comparable effect. In several documented cases, sailing vessels were knocked down to 90°, after which downflooding caused them to sink (Deakin, 1990a; NTSB US, 1987; TSB Canada, 2011). Such scenarios can significantly reduce the effective θ_v. Reflecting this, the IMO (2008a) requires the stability curve to be truncated at the point where downflooding could sink the vessel. This further challenges the value of prescribing a fixed minimum θ_v as a stability criterion.

3.2.2 Initial Metacentric Height

As illustrated in Table 12 most stability standards follow the IS-Code in prescribing $\overline{GM}_0 \geq 0.15\text{m}$, a value derived from statistical analysis of vessel casualty data (IMO, 2008a). A higher value increases the maximum permissible M_H at low angles of heel, which explains the rationale behind elevated $\overline{GM}_0$ criteria of 0.30m and 0.60m. However, no explicit justification is provided for these specific values.

Table 12. $\overline{GM}_0$ criteria.

Criteria		IMO	NK	KR	LR	ABS	DNV W	DNV Y	BV W	BV Y	RINA	REG	USCG
Initial $\overline{GM}$	$\overline{GM}_0 \geq 0.15\text{m}$	X	X	X	X	X					X	X	
	$\overline{GM}_0 \geq 0.30\text{m}$						X		X	X			
	$\overline{GM}_0 \geq 0.60\text{m}$							X					
	Varies												X

The USCG does not prescribe a fixed $\overline{GM}_0$ value and instead considers operating area, vessel type and size, and the upright M_R for bare poles to calculate the minimum required $\overline{GM}_0$. This approach is based on data from conventional sailing vessels (Deakin, 1988), raising some questions about its suitability to modern merchant vessels equipped with mechanical WAPS.

3.2.3 Stability Curve Shape

Even if $\overline{GM}_0$ and the initial stability are sufficient, a vessel may still be vulnerable to capsizing if subjected to a sufficiently strong heeling force (Lewis, 1988). Criteria for $\overline{GZ}$ and the area under the stability curve define the shape of the curve and help ensure that adequate righting moment is available at larger heeling angles. The area criteria further ensure that sufficient righting energy is available to maintain both static and dynamic stability.

Table 13 demonstrates that in most cases no additional criteria are prescribed and stability standards follow those outlined in the IS-Code, particularly when the WAPS is not in operation. The USCG does not define explicit minimum values, these vary depending on vessel characteristics and operating area, but it does require that if $\theta_{\overline{GZ}\max} < 35°$ the stability curve must be truncated at $\overline{GZ}_{35°}$. Only DNV and BV (for yachts) explicitly specify additional $\overline{GZ}$ criteria, which nevertheless differ from each other, further illustrating the lack of a unified approach in this area. Although the use of stricter criteria for WAPS does appear reasonable, no theoretical justification is provided for the specific values applied.

Table 13. Overview of criteria which define the stability curve's shape.

Criteria		IMO	NK	KR	LR	ABS	DNV W	DNV Y	BV W	BV Y	RINA	REG	USCG
Stability Curve Area	$A_{0-30} \geq 0.055$ m rad	X	X	X	X	X	X	X	X	X	X	X	
	$A_{0-40}{}^{*} \geq 0.09$ m rad	X	X	X	X	X	X	X	X	X	X	X	
	$A_{30-40}{}^{*} \geq 0.03$ m rad	X	X	X	X	X	X	X	X	X	X	X	
	Varies												X
$\overline{GZ}$	$\overline{GZ} \geq 0.2\text{m} \ @ \ \theta \geq 30°$	X	X	X	X	X	X	X	X	X	X	X	
	$\overline{GZ}_{\max} \ @ \ \theta \geq 25°$	X	X	X	X	X	X	X	X	X	X	X	
	$\overline{GZ}_{\max} \geq 0.3\text{m}$						X	X					
	$\overline{GZ} \geq 0.5\text{m} \ @ \ \theta \geq 50°$									X			
	Varies												X

3.2.4 Downflooding Angle

An explicit minimum downflooding angle θ_f is not commonly specified for merchant vessels (see Table 14), although it is frequently used as a limiting parameter. Watanabe et al. (1956) proposed that any buoyancy beyond θ_f should no longer be considered effective. This view is replicated in the IS-Code, which defines θ_f as the angle at which significant downflooding occurs. Among the reviewed stability standards, only the REG (2024) explicitly specifies a minimum θ_f, along with a permissible total area of immersed openings prior to θ_f being reached.

Table 14. Downflooding angle criteria.

Criteria		IMO	NK	KR	LR	ABS	DNV W	DNV Y	BV W	BV Y	RINA	REG	USCG
Downflooding angle	–	X	X	X	X	X	X	X	X	X	X		X
	$\theta_f > 40°$											X	

3.2.5 Steady Heel Angle

The maximum permissible θ_S is often defined as a percentage of the angle at which the deck edge becomes immersed, see Table 15, since freeboard is effectively lost at that point and M_R will cease to increase exponentially. Many stability criteria have adopted the IS-Code limit of 16° or 80% of the deck edge immersion angle, a reasonable approach, as the addition of WAPS does not alter the fundamental physical characteristics that determine hull safety. DNV has stated that, in practice, θ_S for WAPS-equipped vessels often remains below 10°, and that a reduced limit would also improve both safety and crew comfort (Mård, 2024). This reflects the fact that WAPS-equipped vessels are subject to sustained heeling angles for longer durations than conventional motor vessels.

Table 15. Steady heel angle criteria.

Criteria		IMO	NK	KR	LR	ABS	DNV W	DNV Y	BV W	BV Y	RINA	REG	USCG
Steady heel	$\leq 16°\ or\ 80\%$	X	X	X	X	X					X		
	$\leq 12°\ or\ 80\%$						X						
	$\leq 20°\ or\ 90\%$								X	X			
	$\leq 20°\ or\ 100\%$							X					
	$\theta_d > 15°$											X	
	Varies												X

The rationale for permitting an increased θ_S is, however, not immediately clear. It may be based on the assumption that sailing vessels are actively operated, allowing for smaller safety margins, or that a lower limit could impose unnecessarily restrictive constraints on vessel design. The WAPS criteria from BV (2025) are ambiguous regarding the specific limit to be applied, as they appear to suggest that the static heel criterion should be evaluated using the maximum gust wind velocity, corresponding to θ_G. If applied in practice, this would result in lower steady heel angles under steady wind conditions, depending on the gust factor, which is however not specified.

The REG (2024) adopts a slightly different approach by introducing the concept of the derived heeling angle θ_d, which is essentially the maximum θ_S up to which the vessel would be safe from downflooding and which should exceed 15°. Deck edge immersion is not utilised as a limiting factor, as it was deemed unsuitable for this purpose (Deakin, 1990a). It remains unclear how a deck edge immersion angle of less than 15° would be addressed.

3.2.6 Dynamic Stability

Figure 12 (A) illustrates the IMO's method for ensuring sufficient dynamic stability, which requires the righting energy (area b), limited by the θ_f, θ_C, or 50°, to at least equal the potential heeling energy (area a) in a scenario where the vessel, having rolled to windward from θ_S with angle θ_1, is struck by a gust. This method is well established, having been applied in historical Japanese and USSR stability standards (Kobylinski & Kastner, 2003; Watanabe et al., 1956), and remains in use across several WAPS stability standards (Table 16). However, several caveats must be considered.

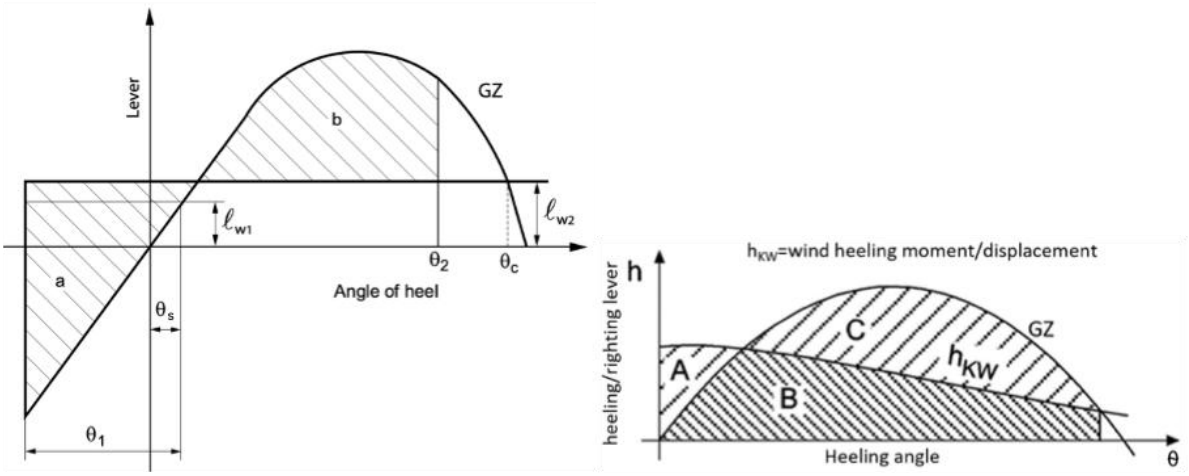

(A) (B)

Figure 12. Illustrations supporting the dynamic stability criteria from the IS-Code (A) and DNV (B) ((A) IMO, 2008a); ((B) DNV, 2025a).

Table 16. Dynamic stability consideration in the stability criteria.

Criteria		IMO	NK	KR	LR	ABS	DNV W	DNV Y	BV W	BV Y	RINA	REG	USCG
Dynamic stability	Energy balance: $A_b/A_a \geq 1.0$	X	X	X	X	X					X		
	Energy balance: $A_B + A_C > 1.4(A_A + A_B)$						X	X					
	$A_{\theta_G - \theta_f} \geq 0.065$ m rad								X	X			
	–											X	
	Varies												X

The IMO's windward roll equation accounts only for vessel characteristics and the viscous hydrodynamic damping effect from underwater appendages, under the assumption that the vessel is drifting beam-on to waves and wind. It does not include either viscous or induced aerodynamic damping from WAPS or other hull-mounted structures, nor does it account for any damping during the leeward roll. Depending on WAPS size and the magnitude of F_Y, the actual windward roll as well as the overshoot past θ_G, discussed by Deakin (1990a), may be significantly less pronounced. Both LR (2025) and DNV (2025b) acknowledge that WAPS can either dampen or amplify rolling motions. However, LR continues to apply the IMO dynamic stability criterion, and DNV (2025b) does not explicitly incorporate these effects for stability as no straightforward analytical method yet exists to quantify them.

Although the DNV stability standard does not explicitly mention it, reference is made to Figure 12 (B) which suggests that DNV assumes the gust is encountered at 0° heel. In this situation, the righting

energy, limited by θ_f or θ_c, is required to exceed the gust wind heeling energy by at least 40%. This approach is also reflected in DNV's yacht criteria (2021) and was historically applied by GL (1996), although both appear to apply the margin using the steady wind heeling lever. This same method was used for the GL-classed WAPS-equipped vessels *Fehn Pollux* (abh, 2018) and *Eship1* (SDC, 2010). This suggests that the original intent of the 40% margin was to account for gusts, a concept also present in the 40% margin proposed by Sarchin and Goldberg (1962), albeit with a different energy balance formulation. This creates ambiguity regarding the purpose and need of DNV's separate gust factor.

The USCG, like the IMO, applies an equivalent energy balance approach, but with several key differences. It is used to verify sufficient dynamic stability to prevent heel beyond θ_f, where the wind heeling energy up to θ_f must equal the total righting energy up to that angle. This method is also used to assess dynamic stability up to θ_v, ensuring it is sufficient to prevent capsizing. If $\theta_v < 90°$, the negative righting energy between θ_v and 90° must also be considered. As is typical of USCG criteria, the vessel's characteristics and operating area play a role in the determination of the exact limits.

In contrast, BV's criteria (2025) do not use the energy balance method to assess dynamic stability. Instead, they require a minimum residual righting energy area between the righting curve and the gust wind heeling curves, as illustrated in Figure 13. The omission of the energy balance method is supported by Deakin (1990a), who observed that heel overshoot beyond θ_G was significantly less than predicted by the traditional energy balance method. This contributed to the rationale for excluding the energy balance method in the REG (2024) criteria. However, this rationale primarily concerns conventional WAPS installations. The dynamic behaviour of vessels equipped with smaller or mechanical WAPS in these conditions remains unclear as no equivalent studies were identified. If such systems offer less aerodynamic damping, effective depowering mechanisms may be required to prevent excessive heel beyond the limits considered in the criteria.

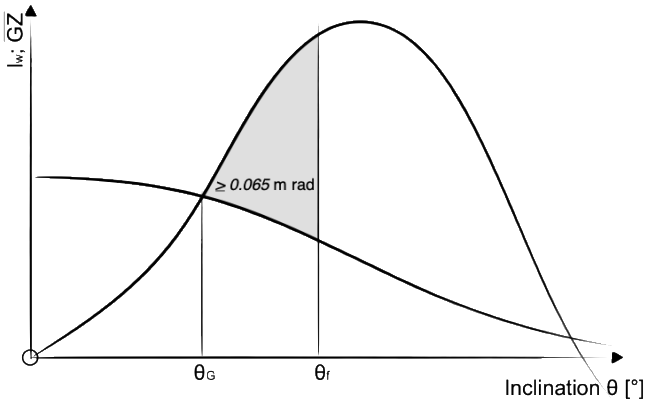

Figure 13. Illustration supporting BV's dynamic stability criterion for wind propelled vessels (BV, 2025).

Additionally, the rationale behind BV's use of a 0.065 m rad value is unclear, and it does not account for specific vessel and WAPS characteristics, raising questions about its validity. Given that BV's yacht criteria (2024a), and earlier BV stability criteria for sailing vessels which considered a larger value (Cleary et al., 1996), do not mention gusts and appear to rely on the steady wind heeling lever it is plausible that the original intent of the minimum residual righting energy area was to accommodate gusts. This raises the possibility that the BV (2025) criteria may account for gusts twice, albeit without explicitly specifying a gust factor.

4. OPERATIONAL STABILITY RISKS

In addition to the lack of a harmonised approach in the criteria and related gaps and inconsistencies, it was also observed that the operational characteristics of WAPS, which play a key role in the actual effect of WAPS on vessel stability, are not always adequately accounted for. This is particularly true for mechanical systems, whose characteristics differ significantly from the more conventional ones upon which many contemporary stability criteria are based.

The maximum C_Y typically occurs when sailing upwind at lower apparent wind angles. Although the exact β at which C_Y is maximised varies with the type of WAPS it generally correlates with the β at which M_H is maximised. In steady conditions, with wind velocity and angle unchanged, the risk of exceeding steady heel limits is limited as it would require the operating crew or system to disregard the increase in vessel inclination. The increase in wind velocity during gusts may result in excessive heel, although its impact varies with WAPS type. Furthermore, other factors, such as rolling motions, broaching, or the use of anti-heeling systems, may also contribute to excessive heeling moments under different conditions.

4.1 Gusts and Depowering

Most stability criteria consider that M_H in a gust increases proportionally to the G_f and a constant C_Y is maintained. For conventional WAPS this is assumed to be a reasonably accurate approximation, although factors such as twist and the stretching of lines and sailcloth may result in the actual behaviour diverging from this assumption. This is however not assumed to have a significant influence, and the inherent dynamic nature of these factors also makes it challenging to accurately predict their impact.

In contrast, the mechanical WAPS do not exhibit a proportional relationship between the G_f and C_Y and the M_H. For Flettner rotors operating at a constant rotational velocity the increase in V_A during a gust would reduce S_R and C_Y, effectively passively depowering the system. Consequently, the actual increase in M_H during a gust can be significantly lower than what the G_f might suggest and depending on the conditions it might even reduce relative to the initial value. Table 17 demonstrates an example for a Flettner rotor with $A_R = 6$ at an apparent wind velocity of 17 m s^{-1} for various apparent wind directions (13.1°; 60.0°; 90.0°) with C_Y peaking at $\beta = 13.1°$. It shows the effect that various gust factors have on a Flettner rotor's C_Y and M_H as a percentage of what the respective values would have been prior to the vessel encountering the gust. The aerodynamic coefficient data are approximated from Vahs (2020) and used to calculate S_R and C_Y both before and after the gust. Considering C_Y and the G_f are the only parameters to change in a gust, the M_H after the gust as a percentage of the initial M_H can be calculated.

Table 17. Table illustrating how a Flettner rotor with a fixed rotational velocity and $A_R = 6$ at a constant β might be affected by a gust with respect to S_R, C_Y, and M_H.

	Before gust			G_f	After gust		
V_A [m s^{-1}]	β [°]	S_R [-]	C_Y [-]	$P(V)$ [-]	S_R [-]	C_Y [-]	M_H
17.0	13.1	2.59	6.89	1.50(1.22)	2.11	4.98(72%)	108%
				2.00(1.40)	1.83	3.86(56%)	112%
				2.25(1.50)	1.72	3.45(50%)	113%
	60.0	2.59	4.71	1.50(1.22)	2.11	3.14(67%)	100%
				2.00(1.40)	1.83	2.33(49%)	99%
				2.25(1.50)	1.72	2.06(44%)	98%
	90.0	2.59	1.56	1.50(1.22)	2.11	0.78(50%)	75%
				2.00(1.40)	1.83	0.46(30%)	59%
				2.25(1.50)	1.72	0.38(24%)	55%

Compared to Flettner rotors, suction sails display similar, albeit less pronounced, behaviour in gusts which can be regarded as a relative passive depowering mechanism. This is due to C_q, which determines the magnitude of the aerodynamic coefficients, being inversely proportional to V_A, as seen in Eq. 2. Table 18, based on figures from Malavard (1984), demonstrates an example of the sub-proportional increase of the wind heeling moment, calculated following the same principle as Table 17 with β, α and Q constant. Due to the lack of publicly available suction sail performance data the aerodynamic coefficient values for $C_q = 0.036$ were assumed to be a suitable approximation of the coefficient values at $C_q = 0.0354$.

Table 18. Table illustrating an example of the effect of a gust on a suction sail, with a fixed α and Q at a constant β, with respect to C_q, C_Y, and M_H.

	Before gust				G_f	After gust		
V_A [m s^{-1}]	β [°]	α [°]	C_q [-]	C_Y [-]	$P(V)$ [-]	C_q [-]	C_Y [-]	M_H
17.0	14.7	30.0	0.05	6.31	2.00(1.40)	0.0354	5.87(93%)	186%
	30.0			6.08			5.64(93%)	185%

In addition to this passive depowering, active measures, which require intervention of crew or control system, may also be employed. For the Flettner rotor this involves decreasing the rotational velocity; for suction sails, the suction flow or angle of attack could be reduced.

A critical advantage of both the passive and the active depowering methods of mechanical WAPS is their fail-safe nature. In scenarios where power is lost or a malfunction occurs, and standard depowering procedures cannot be followed; these systems automatically transition to a safer state without active intervention by for example crew or emergency control systems. For suction sails, this response is nearly instantaneous and stopping the suction flow can reduce C_Y significantly. For example, Table 19, based on data from Kisjes (2017) and Malavard (1984), demonstrates that with $\beta = 15°$ and $\alpha = 15°$, stopping the suction flow in a gust so that $Q = 0$ results in a change from $C_q = 0.05$ to $C_q = 0.00$, reducing C_Y with ~43.8% and resulting in only a minor increase of M_H.

Table 19. Effect of a gust on a suction sail's heeling moment when the suction flow is ceased so that $C_q = 0.05 \rightarrow C_q = 0.00$.

	Before gust				G_f	After gust		
V_A [m s^{-1}]	β [°]	α [°]	C_q [-]	C_Y [-]	$P(V)$ [-]	C_q [-]	C_Y [-]	M_H
15.0	15.0	15.0	0.05	4.70	2.00(1.40)	0.00	2.64(56%)	113%

4.1.1 Fail-safe Depowering Mechanisms

When it is not possible to depower WAPS using the standard operating procedures a fail-safe depowering mechanism is critical to ensure that the system automatically transitions to a safer state without requiring human intervention or active power input and that the initial failure does not increase the risk. The presence of these mechanisms depends largely on the specific characteristics of each system and whether an active force input is required to achieve depowering. Although critical systems may be supplied with emergency electrical power to remain operational, this is not necessarily the case for WAPS.

For Flettner rotors the passive depowering characteristics described above are an excellent fail-safe mechanism. A loss in power in steady conditions would also reduce M_H by gradually decreasing the rotational speed. In some cases redundant electric brakes powered by the system's rotational energy are applied (abh, 2018), enhancing the speed at which the system can be depowered outside of normal operations and if applied automatically when a loss of power is detected presenting a fail-safe method to quickly actively depower the WAPS. The passive fail-safe depowering capability of a

suction sail is in comparison less effective, especially if the suction flow automatically increases during a gust. Nevertheless, a loss in suction flow due to a system failure would be an effective fail-safe active depowering method, significantly reducing M_H. It may be reduced further by aligning the sail with the wind, which is however not a fail-safe mechanism, requiring a resolute action by system or crew.

In contrast, the active methods upon which conventional WAPS rely to depower, reducing sail area, i.e., reefing, or changing the sail angle to reduce α, are not inherently fail-safe and require a power input and active intervention. It would therefore be crucial to integrate these WAPS into the vessel's emergency power grid, or to provide a dedicated uninterruptable power supply, to ensure that in the event of a main power failure it is still possible to actively depower the system. While this is not a fail-safe solution it would enhance the reliability of WAPS depowering in critical situations. Additionally, tailored procedures, crew training, and other mitigation strategies could further reduce associated risks.

In the absence of fail-safe depowering measures, it may also be appropriate to adopt more stringent weather criteria, incorporating larger safety margins. This could also warrant consideration within damage stability assessments, where the absence of an effective fail-safe depowering method might present a critical concern, especially if combined with system failures or a total power loss.

4.1.2 Depowering Through a Heading Change to Windward

Changing vessel heading to windward to reduce β and with a fixed sail angle, α, to depower the WAPS would work for wing-based WAPS (both conventional and suction sails) and was considered by e.g., Perkins et al. (2004) for the Dynarig. This approach would have the added benefit of reducing the hull's lateral force coefficient, further reducing the total M_H, although this effect may vary and would generally be more pronounced with $\beta < 60°$ (Blendermann, 1986, 1993).

However, in cases where the sail angle is changed automatically it may not be as effective. Furthermore, for Flettner rotors α does not play a role in the magnitude of the aerodynamic forces and their C_Y peaks at low β, in which case the WAPS M_H may not notably decrease or initially even increase. Particularly when the system is relatively large this may significantly affect the expected reduction of the total M_H. This makes it clear that depowering through a heading change to windward is not a method which can be universally relied upon as a reliable depowering strategy.

A downwind course presents an alternative method of reducing M_H by reducing both C_Y and V_A. However, additional factors must be considered as downwind courses may induce self-exciting excessive rolling motions (Marchaj, 1996), a phenomenon acknowledged by DNV (2025b) but for which no appropriate quantifying methodology is so far known to have been specified.

4.2 Excessive Heeling Moment Situations

A conventional vessel travelling at a relatively high speed in following or quartering seas develop a directional instability which cannot be countered with the rudder despite maximum steering efforts. Consequently the vessel may broach resulting in an uncontrolled change in heading, leaving the vessel broadside to both wind and waves and vulnerable to capsizing (IMO, 2007, 2008a). Depending on the longitudinal (and in lesser form the lateral) separation between the CE and the CLR, the WAPS's C_Y may generate an additional turning moment (Skogman, 1985). Both on downwind as well as upwind courses this can result in directional instability and increase the likelihood of a broach. Particularly when the WAPS C_Y is relatively large the system can contribute significantly to the likelihood of a broach, although it should be mentioned that longitudinal separation can also be employed as a means to improve a vessel's directional stability.

On a downwind course, C_Y is not maximised and $V_A < V_T$, significantly reducing M_H. Depending on the type of WAPS the F_Y vector may even point to windward, an example of which is illustrated in Figure 14 for the Flettner rotor. Consequently, F_T may be increased compared to an upwind heading in the same conditions. Should the vessel following broach end up beam-on to the wind, V_A and M_H are likely to increase. Combined with the effects of wave action and the internal heeling moment induced by turning (Belenky & Sevastianov, 2007), the total M_H may become significantly higher than expected, underlining the need for effective counter-measures to avoid a broach or quickly depower the WAPS.

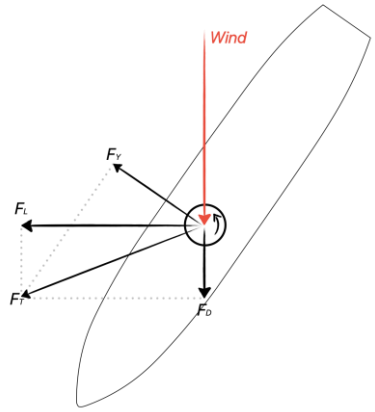

Figure 14. Example of aerodynamic force vectors for the Flettner rotor on a downwind course.

In the event of an upwind broach where the vessel turns to windward the M_H may reduce as described in section 4.1.2. However, its impact across various types of WAPS is not consistent, emphasizing that the system's characteristics are an important factor to be considered and further stressing the importance of effective depowering measures.

The use of WAPS is known to affect manoeuvring characteristics (Vahs et al., 2023), and the potential stability risks arising from manoeuvres conducted while the WAPS is operational require careful further consideration. These manoeuvres may involve substantial course alterations such as tacking (turning the bow through the wind) or gybing (turning the stern through the wind) which may change the direction of M_H or result in a situation where it can increase significantly. Especially with accidental or unsuccessful manoeuvres the stability risks are expected to be greater, given the reduced preparedness.

Following either a successful or an accidental tack or gybe, the vessel may overshoot the intended course. This can result in the vessel becoming beam-on to wind and waves, inducing rolling motions which, combined with the wind-induced heeling moment, may strain the stability. The success of a gybe-manoeuvre is not affected by vessel speed and will, in principle, always succeed. A tacking-manoeuvre is however more likely to be unsuccessful, during which the vessel decelerates significantly, rendering the rudder ineffective and affecting the lateral balance by shifting the CLR aft (Elger et al., 2020). The resulting turning moment may also force the vessel beam-on to the wind and waves. Nevertheless, the risk associated with these manoeuvres is expected to be less pronounced for commercial vessels operating continuous mechanical propulsion which provides additional rudder control even at low vessel speed.

4.3 Anti-Heeling Systems

A method of reducing the static heeling angle when operating WAPS is through the use of anti-heeling systems, typically involving transverse ballast adjustments. Table 20 illustrates which classification societies' stability standards either mention the risk of these systems or provide a methodology to reduce them.

Table 20. Overview of which classification society's stability standards make mention of anti-heeling systems or provide a method to safeguard the potential associated stability risks.

Criteria		IMO	NK	KR	LR	ABS	DNV		BV		RINA	REG	USCG
							W	Y	W	Y			
Anti-heeling system risks	–	X	X	X		X		X		X			X
	Mention				X		X				X	X	
	Method								X				

Both LR and DNV require separate, case-by-case analysis and risk assessments, but do not provide further guidance (DNV, 2025a, 2025b; LR, 2025). The REG (2024), with its emphasis on yachts, outright prohibits the use of such systems. BV (2025) is the sole classification society to provide a more detailed methodology to reduce the risk on stability, based on standards for lifting units (BV, 2015). They require that a vessel must retain sufficient stability in the event of a sudden and complete loss of the wind heeling moment, which could cause a rapid dynamic roll to windward due to the asymmetric ballast distribution from the anti-heeling system.

However, there are several differences between lifting operations and WAPS usage which merit further consideration:

- Operating environment: WAPS are likely to be used in higher wind conditions and rougher sea states than is the case during lifting operations.

- Sudden loss of the heeling moment: BV assumes and instantaneous and absolute reduction of the wind heeling moment. While this may be theoretically possible for some systems, it is in practice likely to be more gradual than the loss of a lifting load.

- Wind direction shift: Perhaps the most critical risk is a reversal of the wind heeling moment direction (e.g., a shift from port to starboard). This could occur due to a steering failure or error, or an upwind broach, and would leave conventional WAPS vessels particularly vulnerable. This risk is currently not addressed and may warrant future consideration.

In the latter case, the combination of wind-induced heel, asymmetric ballast, and beam seas may result in a potentially hazardous stability condition. This scenario, illustrated in Figure 15, has not been explicitly addressed in any of the standards examined. A rapid depowering mechanism could theoretically mitigate this risk, although its effectiveness in such a situation remains uncertain.

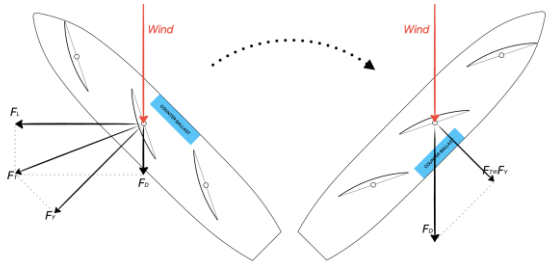

Figure 15. Potential worst-case anti-heeling scenario for 'conventional' WAPS.

For suction sails, the scenario depicted in Figure 15 is assumed to pose less of a risk as these systems would stall, eliminating most aerodynamic lift and due to their smaller sail area the residual drag force would also be limited. However, if the sail angle is adjusted automatically, stalling might be prevented, although it is uncertain if the adjustment would occur quickly enough to create a meaningful stability hazard. It should also be noted that deactivating the suction would lead to a near-instantaneous reduction of M_H which, in combination with transverse-ballast, may induce a sudden heel to windward.

Flettner rotors represent a notable exception, due to their ability to generate lift independent of wind direction, the direction of the force remains unchanged following a wind direction shift. As illustrated in Figure 16, this means that the rotor-generated lateral force would initially continue to counteract the transverse ballast. Nonetheless, if the vessel continues to turn, the lateral force and the ballast-induced heeling moment may eventually act in unison and increase heel. Especially in beam seas this could pose a stability risk. However, the precise impact of Flettner rotors in such a situation remains uncertain and would require further investigation.

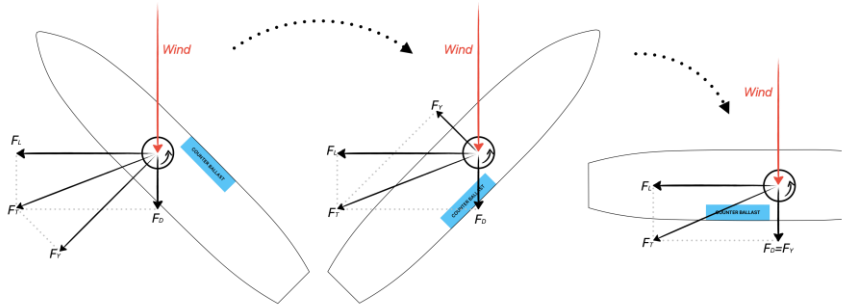

Figure 16. Potential worst-case anti-heeling scenario for Flettner rotors.

An alternative to ballast-based anti-heeling systems can be the use of underwater fins to generate a hydrodynamic righting moment. These could be either in the form of:

- Passive systems, such as the Dynamic Stability System used on yachts, which has been reported to reduce steady heel by up to 34% (Baltic Yachts, n.d.).
- Active fin stabilisers, commonly applied on motor vessels to reduce rolling moments, but potentially adaptable for heel mitigation.

However, in both cases, a sudden loss of this hydrodynamic righting force may leave the vessel with insufficient residual righting moment to counter the wind heeling moment, increasing the risk of a capsize.

5. DISCUSSION

This paper merely addresses the intact stability of wind propelled merchant vessels in a condensed form with the focus primarily on aspects relevant to the characteristics of WAPS. Notably, to maintain brevity, important phenomena such as roll excitation and damping induced by WAPS were only mentioned in passing. These aspects and their influence on vessel stability and related operational risks warrant further exploration.

Since the original study was conducted, several classification societies (LR, DNV, BV, NK, RINA, KR) have published new editions of their wind propulsion standards and stability criteria for WAPS-equipped vessels. After verifying that the content relevant to this paper had not go undergone changes affecting the study or its findings, the references were updated accordingly.

A challenge encountered throughout the process was the lack of clarity and uniformity in stability standards. Discretion was often left to the WAPS manufacturer or vessel designer, requiring several assumptions in their application. This raises the possibility that some criteria may not have been interpreted as intended. Nevertheless, in practical terms, this may be mitigated by direct collaboration between classification societies and manufactures or designers. However, this also introduces the possibility of further deviations or inconsistencies between the various standards.

Additionally, discrepancies between WAPS design load criteria and vessel stability criteria added further complexity. Although some differences may be justified, in certain areas, such as treatment of apparent versus true wind velocities or gust factors, it created some confusion.

6. CONCLUSION

The study has demonstrated that the operational and physical characteristics of WAPS are not comprehensively addressed by current stability standards, particularly regarding modern mechanical systems, which were generally not considered during the development of existing criteria primarily based on conventional WAPS. Gaps and inconsistencies were observed in the stability criteria, where specific limit values frequently lack an explicit theoretical justification, as well as on the potential operational stability risks associated with the use of WAPS. This is compounded by the lack of a unified approach across the various stability standards.

The impact of stability standards was found to vary considerably depending on WAPS type and operational usage with significant variations observed in the magnitude of calculated wind heeling moments. Tailored stability criteria, differentiated by WAPS type or category, could offer significant benefits, especially in relation to gust behaviour and depowering methods. Mechanical systems, in particular, display behaviour that differs substantially from conventional systems. Properly embracing these characteristics could safely enable larger WAPS installations and further optimise their performance. Moreover, especially the dynamic stability behaviour of vessels equipped with smaller or mechanical WAPS requires additional examination.

Several operational stability risks were identified that may lead to significant wind heeling moments beyond the scope of existing methods and assumptions. Special attention should be given to the use of anti-heeling systems. While these are not yet widespread, they can potentially contribute to substantial combined heeling moments and although superficially similar to anti-heeling ballast used in crane lifting operations, the associated operational risks differ and vary by WAPS type. This distinction is not currently reflected in stability standards. Furthermore, the importance of WAPS depowering in reducing the wind heeling moment and stability risks, as well as the respective variations between WAPS types, needs to be considered.

It is thus concluded that the development of stability criteria for WAPS-equipped vessels requires further studying, including criteria tailored to specific WAPS types and their operational behaviour. Both the operational safety and efficiency can benefit from this, which would facilitate and advance the adaptation of wind propulsion technology. Improving the harmonisation and clarity of the criteria would further facilitate the consistency and ease of regulatory compliance.

REFERENCES

abh. (2018). Intact Stability Booklet MV Fehn Pollux. In J. Geterle (Ed.), (Vol. Rev.0 1578-0166). Emden, DE: abh Ingenieur Technik GmbH.

ABS. (2005). Commentary on the Rules for Building and Classing MODU 2001 Pt.3. In: American Bureau of Shipping.

ABS. (2022). Requirements for Wind Assisted Propulsion System installation. In: American Bureau of Shipping.

Anemoi. (2024). Rotor Sail Technology. Retrieved 19-10-2024 from https://anemoimarine.com/rotor-sail-technology/

Baltic Yachts. (n.d.). Dynamic Stability System. https://www.balticyachts.fi/dynamic-stability-system/

BEA MER. (2025). Investigation Report: Foundering of the Schooner De Gallant. https://www.bea-mer.developpement-durable.gouv.fr/IMG/pdf/beamer_rapport_definitif_de_gallant_2025.pdf

Belenky, V. L., & Sevastianov, N. B. (2007). Stability and Safety of Ships: Risk of Capsizing. SNAME.

Blendermann, W. (1986). Die Windkräfte am Schiff. TUHH Schriftenreihe Schiffbau.

Blendermann, W. (1993). Schiffsform und Windlast: Korrelations-und Regressionsanalyse von Windkanalmessungen am Modell. TUHH Schriftenreihe Schiffbau.

Boer, F. (2023). Intact Stability Requirements for Commercial Sailing Vessels, TU Delft. Delft, NL.

Bordogna, G., Keuning, J. A., Huijsmans, R. H. M., Fossati, F. V., & Belloli, M. (2016). Validation of a Simple Aerodynamic Model Capable to Predict the Interaction Effects Occurring Between Two Generic Wind Propulsion Systems. 12th International Conference in Hydrodynamics.

Borg, J. (1986). Magnus Effect: an Overview of its Past and Future Practical Applications, 1850-1985, Volumes 1 and 2. NASA STI/Recon Technical Report N, 86, 30102.

BV. (2015). BV-NR608-DT-R00, Classification of Lifting Units. Bureau Veritas.

BV. (2024a). BV-NR500-Pt.B-DT-R04, Rules for the Classification of Yachts, Pt.B Hull & Stability. Bureau Veritas.

BV. (2024b). Wind Propulsion Technology Report. Bureau Veritas.

BV. (2025). BV-NR206-DT-R03, Wind propulsion systems. Bureau Veritas.

Charrier, B., Constans, J., Cousteau, J.-Y., Daïf, A., Malavard, L., & Quinio, J.-L. (1985). Fondation Cousteau and Eindship Propulsion 1980–1985 System Cousteau-Pechiney. *Journal of Wind Engineering and Industrial Aerodynamics*, 20(1-3), 39-60.

Cleary, C., Daidola, J. C., & Reyling, C. J. (1996). Sailing Ship Intact Stability Criteria. Marine Technology and SNAME News, 33(03), 218-232.

Cousteau, J. Y., Malavard, L., & Charrier, B. (1984). Apparatus for Producing a Force when in a Moving Fluid. https://patents.google.com/patent/US4630997A

Deakin, B. (1988). Sailing Vessel Stability: A Review of the Current State of the Art and Proposals for Worthwhile Research. SNAME, New England Sailing Yacht Symposium, New London, USA.

Deakin, B. (1990a). The Development of Stability Standards for UK Sailing Vessels, RINA, London, UK.

Deakin, B. (1990b). Stability of Sail Training Vessels. *Ship and Boat International*, (5).

Deakin, B. (1991). Model Test Techniques Developed to Investigate the Wind Heeling Characteristics of Sailing Vessels and their Response to Gusts. SNAME, 10th Chesapeake Sailing Yacht Symposium, Annapolis, USA.

Deakin, B. (2009). Stability Regulation of Very Large Sailing Yachts 10th International Conference on Stability of Ships and Ocean Vehicles, St. Petersburg, USA.

DNV. (2021). DNV-RU-YACHT Pt.3 Ch.10. Det Norske Veritas.

DNV. (2024). Wind-Assisted Propulsion Systems, White Paper (How WAPS Can Help to Comply with GHG Regulations. Det Norske Veritas.

DNV. (2025a). DNV-RU-SHIP Pt.6 Ch.2. Det Norske Veritas.

DNV. (2025b). DNV-ST-0511, Wind Asssisted Propulsion Systems. Det Norske Veritas.

Eco Flettner. (2024). Eco Flettner Rotor. Retrieved 12-03-2024 from https://www.ecoflettner.de

Econowind. (n.d.). Ventofoil Operating Principle. https://econowind.nl/how-does-it-work/

Elger, D. E., Bentin, M., & Vahs, M. (2020). Comparison of Different Methods for Predicting the Drift Angle and Rudder Resistance by Wind Propulsion Systems on Ships. *Ocean Engineering*, 217, 108152. https://doi.org/https://doi.org/10.1016/j.oceaneng.2020.108152

EMSA. (2023). Potential of Wind-Assisted Propulsion for Shipping.

Farwind Energy. (2024). Rotor Sail Solutions. Retrieved 19-10-2024 from https://farwind-energy.com/bringing-wind-propulsion-back-to-shipping/

Flettner, A. (1928). Arrangement for Exchanging Energy Between a Current and a Body therein. https://patents.google.com/patent/US1674169A/en

GL. (1996). I - Ship Technology, Pt.3 - Pleasure Craft, Ch.5 Safety Requirements, Sec.3 - Stability. Germanischer Lloyd.

Hsu, S., Meindl, E. A., & Gilhousen, D. B. (1994). Determining the Power-Law Wind-Profile Exponent under Near-Neutral Stability Conditions at Sea. Journal of Applied Meteorology and Climatology, 33(6), 757-765.

Hsu, S.-A. (1988). Coastal Meteorology. Elsevier. ISBN: 9780123579553.

Hu, Y., Tang, J., Xue, S., & Liu, S. (2015). Stability Criterion and its Calculation for Sail-Assisted Ship. *International Journal of Naval Architecture and Ocean Engineering*, 7(1), 1-9.

Hussain, M. D., & Amin, O. M. (2021). A Comprehensive Analysis of the Stability and Powering Performances of a Hard Sail–Assisted Bulk Carrier. *Journal of marine science and application*, 20(3), 426-445.

IMO. (2007). MSC.1/Circ.1228 Revised Guidance to the Master for Avoiding Dangerous Situations in Adverse Weather and Sea Conditions. London, UK: International Maritime Organization.

IMO. (2008a). 2008 International Code on Intact Stability. International Maritime Organization.

IMO. (2008b). Explanatory Notes to the International Code of Stability, 2008. International Maritime Organization.

IWSA. (2024). Wind Propulsion: Zero-Emissions Energy Solution for Shipping - White Paper.

Kisjes, A. (2017). Wind Propulsion for Merchant Vessels: Assesing the Performance of a VentiFoil for Wind Assisted Propulsion TU Delft, NL. Delft, NL. https://resolver.tudelft.nl/uuid:a681c8e6-552e-45a1-8657-893123a8e06b

Kobylinski, L. K., & Kastner, S. (2003). Stability and Safety of Ships. Volume I: Regulation and Operation (R. Bhattacharyya & M. E. McCormick, Eds.)

Kostec. (2024). SV Juren Ae, Final Trim & Stability Calculations.

KR. (2025). Guidance for Prevention Systems of Pollution from Ships. Korean Register.

Kramme, G. (2014). Vergleichende Analyse von Stabilitätskriterien für Schiffe mit Segelantrieben im Rahmen des Projektes “Wind Hybrid Coaster”, University of Applied Sciences Emden-Leer.

Larsson, L., Eliasson, R. E., & Orych, M. (2022). Principles of Yacht Design (A. Coles, Ed.). Bloomsbury Publishing.

Lee, B. S. (2019). Hydrostatics and Stability of Marine Vehicles. Springer.

Lewis, E. V. (1988). Stability and Strength (Vol. 1). The Society of Naval Architects and Marine Engineers.

Lloyd’s list. (2023, 29-11-2023). Top 10 Classification Societies 2023. https://www.lloydslist.com/LL1146894/Top-10-classification-societies-2023

LR. (2025). LR-GN-044, Guidance notes on wind assisted propulsion systems. Lloyd’s Register.

LR. (n.d.). Flettner rotor savings estimator. Lloyd’s Register. Retrieved 19-10-2024 from https://flettner.lr.org/#

Luquet, R., Vonier, P., Leguen, J.-F., & Prior, A. (2015, 14-06-2015). Aerodynamics Loads on a Heeled Ship. 12th International Conference on the Stability of Ships and Ocean Vehicles, Glasgow, UK.

Magnus, G. (1853). On the Deflection of a Projectile. Poggendorf’s Annalen der Physik und Chemie, 88, 804-810.

MAIB. (2025). Interim Report on the Investigation into the Foundering of the Yacht Bayesian. https://assets.publishing.service.gov.uk/media/6821ea1aced319d02c9060f2/2025-Bayesian-InterimReport.pdf

Malavard, L. (1984). Un Nouveau Propulseur Eolien de Navire. La Vie des Sciences, 1, 57-72.

Marchaj, C. A. (1979). Aero-hydrodynamics of Sailing. Adlard Coles.

Marchaj, C. A. (1996). Seaworthiness: The Forgotten Factor. Adlard Coles Nautical.

Mård, N. (2024). Personal DNV correspondence.

MCA. (2004). MGN 280 (M) Construction Standards for Small Vessels in Sport Use. Maritime and Coastguard Agency.

Middendorf, F. L. (1903). Bemastung und Takelung der Schiffe [Masting and Rigging of Ships.

Mohamed Nadzri, M. A. A., & Ahmed, Y. A. (2021). Feasibility Study of Wing Sail Technology for Commercial Ship. *Jurnal Mekanikal,* 26-45.

NK. (2024). Guidelines for Wind-Assisted Propulsion Systems for Ships (Edition 2.1). Nippon Kaiji Kyokai.

Norsepower. (2024). Rotor Sail Technical specifications. Vol. 2024. Helsinki, Finland.

NTSB US. (1987). Marine Accident Report, Capsizing and Sinking of the US SV Pride of Baltimore (NTSB/MAR-87/01).
https://ntrl.ntis.gov/NTRL/dashboard/searchResults/titleDetail/PB87916401.xhtml

Okada, S. (1952). On the Heeling Moment due to the Wind Pressure on Small Vessels. *Journal of the Society of Naval Architects of Japan*, 1952(92), 75-81.

Oossanen, P. v. (1997). Development of Proposed ISO 12217 Single Stability Index for Mono-Hull Sailing Craft. SNAME, 13th Chesapeake Sailing Yacht Symposium, Annapolis, USA.

Perkins, T., Dijkstra, G., & Roberts, D. (2004). The Maltese Falcon: The Realisation 22nd International HISWA Symposium on Yacht Design and Yacht Construction,

REG. (2024). Part B, Passenger Yacht Code. Red Ensign Group.

RINA. (2025). RINA-REP6-Pt.F. In Wind Assisted Propulsion Systems: Registro Italiano Naval.

Sarchin, T. H., & Goldberg, L. L. (1962). Stability and Buoyancy Criteria for US Naval Surface Ships SNAME, Meeting, Washington DC, USA.

Sato, M., Yamanouchi, Y., Motora, S., & Uchida, M. (1954). A Proposed Standard of Stability for Passenger Ship Part I: Smooth Water Area. Journal of Zosen Kiokai, 1954(95), 65-80.

Schenzle, P. (1985a). Indosail project windforce coefficients.

Schenzle, P. (1985b). The 'Indosail' project. *Journal of Wind Engineering and Industrial Aerodynamics* 19, 19-43.

SDC. (2010). MV E-ship 1, Intact Stability Information & Calculations. Hamburg, DE: Ship Design & Consult GmbH.

SDC. (2021). Juren Ae Project Intact Stability Calculation. Hamburg, DE: Ship Design & Consult GmbH.

Skogman, A. (1985). The Practical Meaning of Lateral Balance for a Sail-Assisted Research Vessel. *Journal of Wind Engineering and Industrial Aerodynamics*, 20(1), 201-226. https://doi.org/https://doi.org/10.1016/0167-6105(85)90019-4

Swanson, W. (1961). The Magnus Effect: A summary of Investigations to Date. *Journal of Basic Engineering*. https://doi.org/10.1115/1.3659004

TSB Canada. (2011). Knockdown & Capsizing of the Sail Training Yacht Concordia (M10F0003). Minister of Public Works and Government Services Canada. https://www.tsb.gc.ca/eng/rapports-reports/marine/2010/m10f0003/m10f0003.html

USCG. (n.d.-a). Calculation of wind heeling moments Mobile Offshore Drilling Units. In (Vol. 46 CFR 174.055).

USCG. (n.d.-b). Subchapter S - Subdivision and Stability. In (Vol. 46 CFR Part 170-174).

Vahs, M. (2020). Retrofitting of Flettner Rotors–Results from Sea Trials of the General Cargo Ship “Fehn Pollux”. *International Journal of Maritime Engineering*, 162(A4).

Vahs, M., Wagner, S., & Strasser, S. (2023). Navigating and Manoeuvring of Modern Wind Powered Ships STAB/ISSW, 19th International Ship Stability Workshop, Istanbul, Turkey. https://www.researchgate.net/publication/375237781_Navigating_and_Manoeuvring_of_modern_Wind_powered_Ships

Wagner, B. (1967). Windkanalversuche für einen sechsmastigen Segler nach Prölss. TUHH Schriftenreihe Schiffbau.

Watanabe, Y., Inoue, S., Yamanouchi, Y., Manabe, D., Kato, H., Sato, M., Motora, S., Masuda, Y., & Uchida, M. (1956). A Proposed Standard of Stability for Passenger Ships. *Journal of Society of Naval Architects of Japan*, 99, 29-46.

Wendel, K. (1959). Safety from Capsizing. Fishing Boats of the World 2: Sea Behaviours, Second Fishing Boats Congress, Rome, Italy.

Wolfson Unit. (2006). Research Project 534, Stability Criteria for Large Sailing Yachts (Report No. 1924).